JOBNAME: JHM 00#00 2018 PAGE: 1 SESS: 8 OUTPUT: Mon Feb 19 16:26:22 2018 Total No. of Pages: 14
/ams/jhm/0/jhmD170078



Journal of Hydrometeorology (Proof Only)

# On the Role of NAO-Driven Interannual Variability in Rainfall Seasonality on Water Resources and Hydrologic Design in a Typical Mediterranean Basin

ROBERTO CORONA AND NICOLA MONTALDO

*Dipartimento di Ingegneria Civile, Ambientale e Architettura, Università di Cagliari, Cagliari, Italy*

JOHN D. ALBERTSON

*School of Civil and Environmental Engineering, Cornell University, Ithaca, New York*

(Manuscript received 24 April 2017, in final form 3 November 2017)

ABSTRACT

In the last several decades, extended dry periods have affected the Mediterranean area with dramatic impacts on water resources. Climate models are predicting further warming, with negative effects on water availability. The authors analyze the hydroclimatic tendencies of a typical Mediterranean basin, the Flumendosa basin located in Sardinia, an island in the center of the Mediterranean Sea, where in the last 30 years a sequence of dry periods has seriously impacted the water management system. Interestingly, in the historic record the annual runoff reductions have been more pronounced than the annual precipitation reductions. This paper performs an analysis that links this runoff decrease to changes in the total annual precipitation and its seasonal structure. The seasonality is a key determinant of the surface runoff process, as it reflects the degree to which rainfall is concentrated during the winter. The observed reductions in winter precipitation are shown here to be well correlated (Pearson correlation coefficient of −0.5) with the North Atlantic Oscillation (NAO) index. Considering the predictability of the winter NAO, there is by extension an opportunity to predict future winter precipitation and runoff tendencies. The recent hydroclimatic trends are shown to impact hydrologic design criteria for water resources planning. The authors demonstrate that there is a dangerous increase of the drought severity viewed from the perspective of water resources planning.

AU1

## 1. Introduction

Over the past several decades extended dry periods have affected the Mediterranean regions with notable effects on agriculture and water resources (Piervitali et al. 1999; Brunetti et al. 2001, 2002; Dai et al. 2004; García-Ruiz et al. 2011; López-Moreno et al. 2011; Vicente-Serrano et al. 2011; Altın and Barak 2014), and future drier trends have been predicted by climate models over the Mediterranean basin (May 2008; Mariotti et al. 2008; Ozturk et al. 2015).

Significant negative trends have been detected for river flow time series over many Mediterranean regions, including the Iberian Peninsula (López-Moreno et al. 2008; García-Ruiz et al. 2011; Lorenzo-Lacruz et al. 2012; Martínez-Fernández et al. 2013), the Italian Tiber River (Romano et al. 2011), and areas of France (Lespinas et al. 2010). Lorenzo-Lacruz et al. (2012) highlighted significant negative trends for discharges in winter and spring mainly, for almost all of the examined Iberian rivers. The position of the island of Sardinia, in the center of the western Mediterranean basin, with its low level of both urbanization and human activity help make Sardinia an excellent reference laboratory of Mediterranean ecosystem studies and provides a general lens on the recent negative trends detected in Mediterranean areas.

In the Flumendosa basin, a key basin of the Sardinian water resources system, the average annual runoff in the latter part of the twentieth century was less than 65% of the historic average value (Fig. 1a; mean runoff for years 1923–74 was $426 \times 10^6\,m^3$, while mean runoff for the years 1975–2007 was $276 \times 10^6\,m^3$ over the $934\,km^2$ basin), reaching extremely low values of yearly runoff in 1995 ($= 56 \times 10^6\,m^3$) and 2002 ($= 36 \times 10^6\,m^3$). This strong runoff reduction dramatically impacted agricultural water use and even the domestic water use (Statzu and Strazzera 2009), since the reservoir system of the

F1

*Corresponding author*: Roberto Corona, roberto.corona@unica.it

DOI: 10.1175/JHM-D-17-0078.1

JOBNAME: JHM 00#00 2018 PAGE: 2 SESS: 8 OUTPUT: Mon Feb 19 16:26:22 2018 Total No. of Pages: 14
/ams/jhm/0/jhmD170078





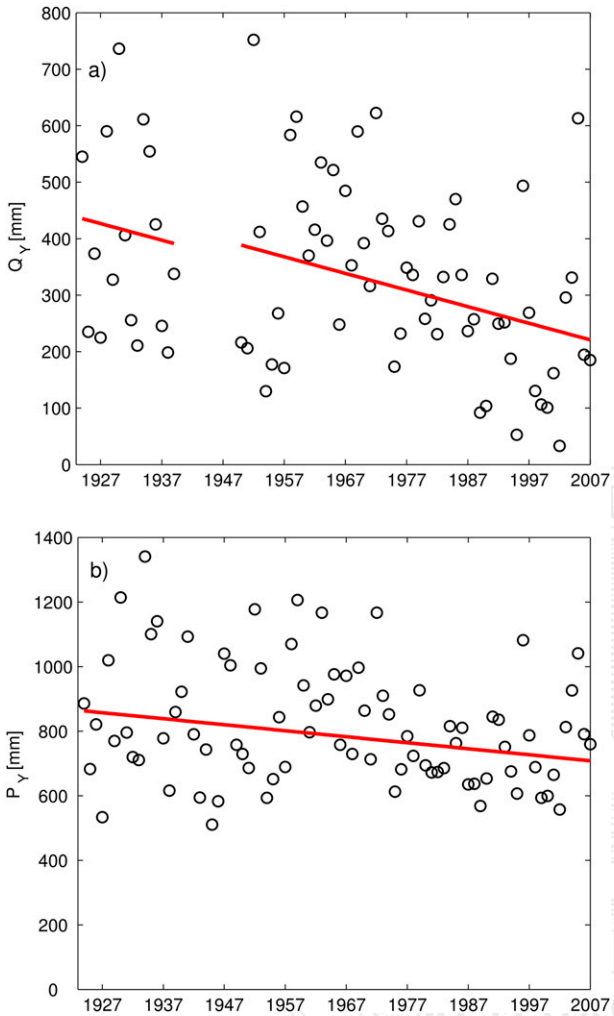


FIG. 1. Time series of the yearly totals at basin scale of (a) runoff $Q_Y$ and (b) rainfall $P_Y$. For each plot the red line represents the slope of the temporal trend estimated with the nonparametric TSA.

Flumendosa River supplies the water needs of much of southern Sardinia, including the island's largest city, Cagliari (about 450 000 inhabitants in the metropolitan area).

The reduction in annual precipitation of the Flumendosa basin (Fig. 1b; a decrease on average of 16% in the last 33 years) has not been as drastic as with the discharge, suggesting a high precipitation elasticity of streamflow [$\varepsilon_p = (dQ/Q)/(dP/P)$, where $Q$ is runoff and $P$ is precipitation], which is an indicator often considered when evaluating the impact of climate change on runoff (Schaake and Chunzhen 1989; Sankarasubramanian et al. 2001).

A framework for evaluating the relation between changes of annual precipitation and runoff was well defined by Roderick and Farquhar (2011) and, more recently, Zhou et al. (2016), who build on the runoff climate elasticity concept and the Budyko functions (Choudhury 1999) to derive the change of the mean annual runoff $Q_Y$ due to the changes in climate (annual precipitation $P_Y$ and potential evaporation $E_p$) and catchment properties $c$ using a first-order Taylor approximation of the total differential:

$$dQ_Y = \frac{\partial Q_Y}{\partial P_Y}\, dP_Y + \frac{\partial Q_Y}{\partial E_p}\, dE_p + \frac{\partial Q_Y}{\partial c}\, dc, \qquad (1)$$

where the partial derivatives represent the sensitivity of runoff to precipitation, to potential evapotranspiration, and to the changes in the basin as result of human activities. In the Flumendosa basin, the influence of $E_p$ on runoff is negligible as the changes in air temperature (which is a key term of $E_p$; e.g., Maidment 1993) have been much less severe than the changes in rainfall, and the changes of basin characteristics are negligible, leaving the changes of precipitation as the dominant driver. The errors in the use of (1) may be significant, such as evaluated by Yang et al. (2014) through a comparison of (1) with the complete Taylor expansion for 207 catchments in China over the period from 1961 to 2010 considering only the sensitivity to $E_p$ and $P_Y$. In Mediterranean climates, which are characterized by strong seasonality with cool, wet winters and hot, dry summers (Barry and Chorley 1992; Lionello et al. 2006), the first-order Taylor approximation may be even more problematic.

In Mediterranean climates, the seasonality of the precipitation needs to be considered. During the rainy seasons $E_p$ is low and during the dry season it is high, such that rain is out of phase with $E_p$, and runoff is mainly driven by the fraction of precipitation received during the rainy season. Therefore, seasonal shifts in rainfall impact the runoff (e.g., with a shift of rain from winter to spring, runoff will decrease because of higher $E_p$). Here we evaluate the role of precipitation seasonality and the impact of the seasonality precipitation change on the runoff through the use of a seasonality index (Markham 1970), which provides a measure of both the disbalance of precipitation across the seasons and the period where the precipitation is most strongly concentrated.

The seasonal structure of precipitation and its interannual variability are key points for the Mediterranean water resources system sustainability, as wet months are needed to provide reserves for the subsequent dry seasons (e.g., Montaldo et al. 2008). The surface runoff plays a central role in water resources planning systems for these water-limited regions (García-Ruiz et al. 2011). In the Mediterranean basin, this strong seasonality is mainly controlled by atmospheric circulation patterns,

JOBNAME: JHM 00#00 2018 PAGE: 3 SESS: 8 OUTPUT: Mon Feb 19 16:26:22 2018 Total No. of Pages: 14
/ams/jhm/0/jhmD170078





most notably a strong subtropical high pressure cell that persists in the summer months, and its persistence is essential for future water resources sustainability, while the cold/wet season is affected by the arrival of midlatitude westerlies (Rojas et al. 2013). In addition to the areas in and surrounding the Mediterranean Sea, this type of climate prevails in parts of western North America, South America, Western and South Australia, and sub-Saharan Africa (Doblas-Miranda et al. 2015), further increasing the importance and generality of this study.

Delitala et al. (2000) and Dunkeloh and Jacobeit (2003) observed a drastic reduction of winter and spring precipitation in Sardinia and Mediterranean regions due to circulation pattern changes over time. Much effort has been focused on the relationship between winter precipitation and large-scale pressure indices for the Mediterranean regions (Osborn et al. 1999; Trigo et al. 2000; Brunetti et al. 2001; Trigo and Palutikof 2001; Brunetti et al. 2002; Dunkeloh and Jacobeit 2003; López-Moreno et al. 2011; Rojas et al. 2013), with a picture emerging (Lionello et al. 2006) that ties winter precipitation dynamics to the winter North Atlantic Oscillation (NAO) index dynamics in the Mediterranean basin. The NAO is defined as the normalized pressure difference between a station in the Azores and one in Iceland (Hurrell 1995). The NAO affects the orientation of the air flow, thus exerting a control on the branch of storm tracks affecting the Mediterranean area. Hurrell (1995) demonstrated a clear connection between the persistent positive phase of the NAO and precipitation reduction in the Mediterranean area as storm tracks and moisture transport from the Atlantic are directed more toward northern Europe, with a corresponding reduction of the total moisture transport over the Mediterranean area.

The position of Sardinia in the center of the western Mediterranean provides a useful test on the influence of the NAO on the Mediterranean climate regime. The Sardinian climate is connected to large-scale circulation structures, especially westward by the North Atlantic (Delitala et al. 2000). This underlies the results of Delitala et al. (2000), who found a Pearson correlation coefficient of $-0.5$ ($p < 0.001$) between an index of the NAO and precipitation anomalies in the months of October–April (1946–93). Delitala et al. (2000), however, did not investigate the impact of this relationship on trends in precipitation and their consequence on runoff. Here we investigate the connections of winter precipitation and runoff with the major circulation indexes (e.g., NAO) for evaluating the role of the atmospheric circulation patterns on the recent dry periods in the Sardinian basin.

The Flumendosa basin is well suited to this analysis thanks to low human activities (only 0.8% of the territory is urbanized) and the large hydrological database (1922–2007 period). Specifically, we address the objectives of 1) investigating the role of the precipitation seasonality on runoff of the Flumendosa basin, 2) unraveling the influence of the NAO on precipitation and runoff changes over the instrumented period, and 3) investigating the potential implications of climate change effects on hydrological planning and designs, both under the water resources planning perspectives (Chiew et al. 2011).

## 2. Data and methods

### a. The Flumendosa basin

The Flumendosa basin is located in central-eastern Sardinia, and Flumendosa is the second-longest river of the region with a length of 127 km. The northern part of the basin is mountainous with steep hillslopes and higher rainfall compared to the southern part. Two large dams, the Flumendosa Dam at Nuraghe Arrubiu (reservoir capacity of $300 \times 10^6\,m^3$) and the Mulargia Dam at Monte Su Rei, (reservoir capacity of $320 \times 10^6\,m^3$), collect runoff from a basin area of $934\,km^2$ (Fig. 2). The F2
two reservoirs are interconnected with an underground conduit to increase the collection of the runoff coming from the Nuraghe Arrubiu dam basin, which is much larger than the Mulargia basin ($170\,km^2$), so that total capacity of the reservoir systems is $620 \times 10^6\,m^3$, one of the highest reservoir capacities in Europe. Because of its key role in the Sardinian water resources system, the Flumendosa basin became an experimental basin of the University of Cagliari (Detto et al. 2006; Montaldo et al. 2008, 2013), resulting in an extensive hydrological database.

The climate regime is typically Mediterranean. The mean annual precipitation (1922–2007) is 819 mm with strong seasonality and interannual variability: the mean historical monthly precipitation ranges from 9 mm in July to 124 mm in December. The mean historical monthly temperature ranges from a minimum of 7.1°C in January to a maximum of 23.7°C in July.

The soil thickness in the basin generally ranges from 5 to 80 cm with an average depth of <50 cm; the soil texture is mainly silt loam soils in the valley with the mountainous part dominated by exposed rocks. The land use is also inhomogeneous with forested and natural areas predominant in the north, while in the south (downstream) agriculture practice activities and grazing areas are common due to thicker soils.

### b. Methods

Daily precipitation data from 31 rain gauge stations in and surrounding the Flumendosa basin and monthly

JOBNAME: JHM 00#00 2018 PAGE: 4 SESS: 8 OUTPUT: Mon Feb 19 16:26:23 2018 Total No. of Pages: 14
/ams/jhm/0/jhmD170078



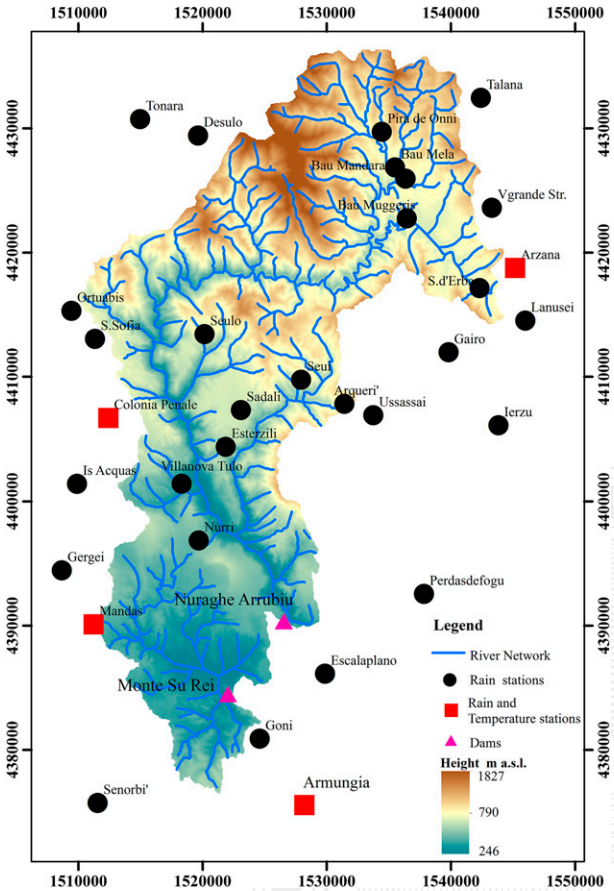


FIG. 2. The Flumendosa River basin with the position of the rain gauges, the temperature stations, and the two dams identified.

runoff data at the basin outlet were collected for the period 1923–2007 (Fig. 2). Runoff has been monitored through a discharge gauge station of the Sardinian Regional Hydrographic Service. When the reservoirs started to operate (in 1960), the Ente Acque della Sardegna (ENAS) authority has estimated monthly runoff values through the reservoir water balance [properly calibrated and validated by ENAS and Cao et al. (1998)]. Air temperature data of eight stations are available at the monthly scale (Fig. 2), but only four stations are included in the study because only these stations exhibit continuous observations for a time period greater than 50 years.

Statistics were computed and analyzed on the annual and monthly time series of precipitation, runoff, and temperature. Spatially mean rainfall data were estimated using the Thiessen method (Thiessen 1911). Temporal trends were estimated using the nonparametric Mann–Kendall (MK) test (Helsel and Hirsch 2002), which provides a $\tau$ value that is a robust measure of the strength of the trend with values ranging from −1 (maximum decrease in time) to +1 (maximum increase in time) and also its significance level (details in appendix A). The Theil–Sen approach (TSA; appendix B; Theil 1950; Sen 1968), a common nonparametric method, is used for estimating the slope of the trend line.

We also used the nonparametric Pettitt's test (Pettitt 1979), widely used in climatic records (Zhang and Lu 2009; Gao et al. 2011; Jaiswal et al. 2015), for estimating potential changepoints of the annual runoff time series.

We use the monthly NAO index time series of Hurrell (1995) available from 1864 onward. For more regional indicators of pressure anomalies in the Mediterranean basin, two alternative forms of the Mediterranean Oscillation Index (MOI_1 and MOI_2) have been also collected from the Climatic Research Unit database: MOI_1 represents the normalized pressure difference between Algiers and Cairo while MOI_2 is between Israel and Gibraltar (Conte et al. 1989).

Time series of the extended winter (December–March) average indices of the NAO and MOI were derived ($NAO_W$, $MOI1_W$, and $MOI2_W$). The correlation between winter values of the circulation indices and winter precipitation have been evaluated using the Pearson correlation coefficient, widely used for hydrologic studies (Dunkeloh and Jacobeit 2003; Brandimarte et al. 2011; López-Moreno et al. 2011).

For evaluating the seasonality of rain time series, we use the seasonality index of Markham (1970). In the Markham method (Markham 1970) monthly rainfall values are assembled as vector quantities, where the magnitude is the amount of rain in a month $p_m$ (where $m = 1, 2, \ldots, 12$ are the months of the year) and the direction corresponds to the month of the year expressed by the angle $\alpha_m$, measured clockwise from January (Dingman 2015). The vector resultant over the year is a measure of rainfall seasonality, with the magnitude representing the degree of seasonality and the angle $\omega$ pointing to the dominant rainfall period:

$$\omega = \arctan \frac{\sum_{m=1}^{12} p_m \cos\alpha_m}{\sum_{m=1}^{12} p_m \sin\alpha_m}. \quad (2)$$

For example, the climatological mean annual cycle of monthly rainfall and the resultant vector for the Flumendosa basin (1922–2007 period) are reported in Fig. 3, showing that the resultant vector direction $\omega$ is 5.88°, which, converted to a time direction, is 6 January (the date of concentration is calculated by adding the number of days from the beginning of the year). The seasonality index (SI) is the ratio between the

JOBNAME: JHM 00#00 2018 PAGE: 5 SESS: 8 OUTPUT: Mon Feb 19 16:26:23 2018 Total No. of Pages: 14
/ams/jhm/0/jhmD170078



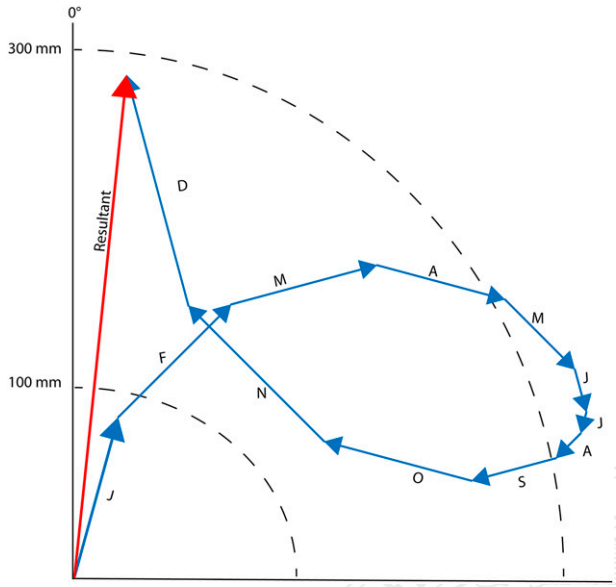


FIG. 3. Vectorial mean monthly rainfall and the resultant vector at the Flumendosa basin.

magnitude of the resultant vector $P_r$ and the total annual precipitation $P_Y$:

$$\mathrm{SI} = \frac{P_r}{P_Y}, \tag{3}$$

where

$$P_r = \sqrt{\left(\sum_{m=1}^{12} p_m \cos\alpha_m\right)^2 + \left(\sum_{m=1}^{12} p_m \sin\alpha_m\right)^2}. \tag{4}$$

The values of the seasonality index are between 0 and 1. The maximum possible SI value would occur for a case where the total annual precipitation was concentrated in a single month. Note that the seasonality index for the climatological mean seasonal cycle of the Flumendosa basin is 0.34 ($P_r$ = 279.21 mm and $P_Y$ = 818.82 mm; Fig. 3).

The recent precipitation decreases in this region may have important implications for water resources planning and design. For investigating the potential implications of the increase of dry periods, whose length is expected to further increase in the future in the Mediterranean area (Beniston et al. 2007), we make use of the drought severity index (DSI; ~~Yievchev~~ 1967; Dracup et al. 1980; Clausen and Pearson 1995). Hydrological droughts are usually identified by monthly runoff $Q_M$ time series through the truncation level approach, which assumes that droughts are periods during which the discharges are lower than a threshold discharge $Q_{95}$ (~~Yievchev~~ 1967; Dracup et al. 1980; Clausen et al. 1995; Mishra and Singh 2010; Wanders and Wada 2015), which is the 95th percentile of historical runoff time series (1923–2007; Zelenhasić and Salvai 1987; Chang and Stenson 1990). In this way, the drought condition (Dc) is

$$\mathrm{Dc} = \begin{cases} 1 & \text{for} \quad Q_M < Q_{95} \\ 0 & \text{for} \quad Q_M \geq Q_{95} \end{cases}. \tag{5}$$

The statistical properties of a drought are the duration, severity, and intensity (Yevjevich 1967; Mishra and Singh 2010), which can be summarized by the DSI, which is the cumulated deficit of runoff below the fixed threshold discharge (~~Yievchev~~ 1967; Dracup et al. 1980; Clausen and Pearson 1995).

TABLE 1. For seasonal and annual precipitation ($P_S$ and $P_Y$, respectively) and runoff ($Q_S$ and $Q_Y$, respectively), the MK $\tau$ values ($\tau_P$ and $\tau_Q$) and the slopes estimated using the TSA ($\beta_P$ and $\beta_Q$), the precipitation elasticities to streamflow ($\varepsilon_P$ and $\varepsilon_Q$), and the temporal mean ($\overline{P}$ and $\overline{Q}$), and the ratios between total seasonal runoff and total yearly runoff ($Q_S/Q_Y$), the ratios between seasonal rain and yearly rain ($P_S/P_Y$), the ratios between $\beta_P$ and $\overline{P}$, and the ratios between $\beta_Q$ and $\overline{Q}$.

| | JFM | AMJ | JAS | OND | Year |
|---|---|---|---|---|---|
| $P_S/P_Y$ | 0.32 | 0.19 | 0.10 | 0.39 | — |
| $Q_S/Q_Y$ | 0.52 | 0.18 | 0.02 | 0.28 | — |
| $\varepsilon_P$ | 1.15 | 1.36 | 0.55 | 1.97 | 2.18 |
| $\tau_P$ | −0.21 | 0.01 | 0.14 | −0.13 | −0.20 |
| $\tau_Q$ | −0.23 | −0.12 | −0.22 | −0.20 | −0.25 |
| $\beta_P$ (mm yr$^{-1}$) | −1.45 | 0.05 | 0.40 | −1.00 | −1.80 |
| $\beta_Q$ (mm yr$^{-1}$) | −1.44 | −0.31 | −0.0578 | −0.77 | −2.94 |
| $\overline{P}$ (mm) | 263.32 | 152.55 | 80.03 | 322.92 | 818.82 |
| $\overline{Q}$ (mm) | 173.56 | 61.92 | 5.71 | 95.25 | 336.45 |
| $\beta_P/\overline{P}$ (yr$^{-1}$) | −0.0055 | 0.0003 | 0.0050 | −0.0031 | −0.0022 |
| $\beta_Q/\overline{Q}$ (yr$^{-1}$) | −0.0083 | −0.0051 | −0.0101 | −0.0081 | −0.0087 |

## 3. Results

### a. Annual trends of hydrological time series

The Flumendosa basin runoff has decreased significantly (Fig. 1), with an MK $\tau$ value of −0.25 (with $p <$ 0.001) and a slope of the trend line, derived using the TSA (see appendix B) of −2.94 mm yr$^{-1}$ (Table 1).

Few hydrologic years were dry in the first five decades of the studied period, such as years in the 1924–40 period with a minimum runoff value of 198.6 mm, but the driest and longest dry conditions were in the last three decades, starting mainly from 1975. Indeed, 1975 was the first "warning" year for the Flumendosa water resources system management with runoff values lower than 173 mm, followed first by a decade of low runoff values (persistently below the 1923–74 average of 400 mm), and then by the driest last two decades characterized by 6 years with runoff < 100 mm (Fig. 1). The year 1975 is

JOBNAME: JHM 00#00 2018 PAGE: 6 SESS: 8 OUTPUT: Mon Feb 19 16:26:23 2018 Total No. of Pages: 14
/ams/jhm/0/jhmD170078





confirmed statistically to be a changepoint of the runoff time series by the Pettitt's test widely used in climate records (Pettitt 1979; Zhang and Lu 2009; Gao et al. 2011; Jaiswal et al. 2015). While two potential changepoints are estimated, the years 1986 and 1975, (with $p < 0.001$ for both years), we consider the year 1975 as a useful focal point for analysis as it divides the times series into two subperiods of near-identical lengths. Low runoff (the minimum amount ~33 mm; Fig. 1a), reduced the water availability for domestic uses in the Sardinian capital of Cagliari, where in the 2002 summer water restrictions were initiated that reduced the domestic water supply to 6 h day$^{-1}$. Note that, unfortunately, runoff data are missing for the period 1940–48 because of the lack of the national Hydrographic Office during World War II.

The annual temperature trend is not statistically significant (MK $\tau$ of $-0.02$, with $p > 0.1$), and recalling that the surface solar radiation trend is also not statistically significant during the period 1959–2013 over the south area of Italy (Manara et al. 2016), low historical changes of $E_p$ (which is highly related to air temperature; e.g., Maidment 1993) can be deduced and, therefore, the weight of $dE_p$ on the runoff changes estimated with (1) is negligible.

The precipitation trend is significantly negative but with lower values (the MK value of $\tau$ is $-0.2$, $P < 0.01$, while the trend line slope is $-1.8$ mm yr$^{-1}$) than for the runoff. The value of the precipitation elasticity of streamflow (Sankarasubramanian et al. 2001) is rather high at 2.18, such that a 10% change in precipitation results in a runoff change of 21.8%, for example.

The annual runoff coefficient ($\phi_Y = Q_Y/P_Y$) trend is negative, with an MK $\tau$ value of $-0.25$ ($p < 0.01$) and a trend line slope of 0.003 yr$^{-1}$ (Fig. 4). The last several decades have seen the lowest $\phi_Y$ values (mostly <0.3) of the analyzed period, while the yearly precipitation values are not so extremely low in the same period.

We note a strong relationship between $\phi_Y$ and $P_Y$ for this case study (Fig. 5, correlation coefficient of 0.71). The relationship between $P_Y$ and $\phi_Y$ is nonlinear and can be estimated with an inverse relationship expressed as follows:

$$\hat{\phi}_{Y_1} = a_1 P_Y^{-1} + b_1, \tag{6}$$

where $\hat{\phi}_{Y_1}$ is the value of $\phi_Y$ estimated using the annual total rainfall $P_Y$ and (6), and $a_1$ and $b_1$ are the regression coefficients ($a_1 = -349.8$ mm and $b_1 = 0.84$). The value of the coefficient of determination $R^2$ is 0.5 while the root-mean-square error (RMSE) value is 0.09. A large scatter of $\phi_Y$ values about the regression line is observed for the full range of rainfall values (Fig. 5), which we hypothesize

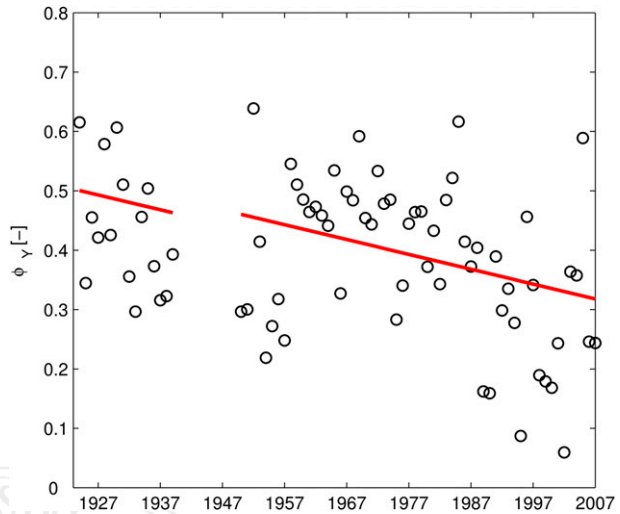


FIG. 4. Yearly totals of the runoff coefficient (total discharge/total precipitation). The red line is the slope of the temporal trend estimated with the nonparametric TSA.

is largely due to the variability of the precipitation during the year (i.e., interannual variability in seasonality).

In fact, the seasonal runoff coefficient ($\phi_S = Q_S/P_S$, with $Q_S$ being the seasonal runoff and $P_S$ being the seasonal precipitation) shows a considerable variability (Fig. 6), with the highest values during winter (January–March) when the $E_p$ is low, the soil moisture is naturally high, and the surface runoff process is enhanced. Instead, during summer and autumn (July–September and October–December, respectively) the values of $\phi_S$ are low due predominantly to the dry antecedent soil moisture conditions—owing both to lower seasonal rainfall inputs and higher $E_p$.

The total annual runoff depends on how precipitation is distributed across the seasons: in the 1950/51 and 1936/37 hydrologic years the precipitation amounts were similar (1178 and 1140 mm, respectively) while $\phi_Y$ values were quite different (0.64 and 0.37, respectively). The reason was that the precipitation of the 1950/51 hydrologic year was mainly concentrated during the wet period (winter precipitation of 1037 mm) while the precipitation of the 1936/37 hydrologic year was more uniformly distributed during the year (e.g., the precipitation was of 537 mm in spring and summer).

The influence of the precipitation seasonality on the runoff coefficient is suggested by Fig. 7, where $\phi_Y$ is examined against the standard deviation of monthly precipitation of each year [Std($P_M$)] in the study period [$\mathrm{Std}(P_M) = \sqrt{(1/12)\sum_{m=1}^{12}(p_m - \overline{p}_m)^2}$, where $\overline{p}_M$ is the total monthly precipitation of a given year]. The relationship between Std($P_M$) and $\phi_Y$ is estimated with an inverse relationship expressed as follows:

JOBNAME: JHM 00#00 2018 PAGE: 7 SESS: 8 OUTPUT: Mon Feb 19 16:26:24 2018 Total No. of Pages: 14
/ams/jhm/0/jhmD170078



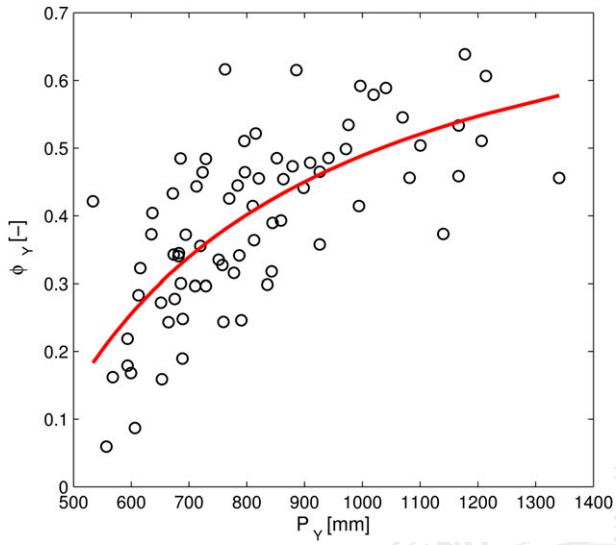


FIG. 5. Annual runoff coefficient $\phi_Y$ vs the annual precipitation $P_Y$. Observed values are in black open circles and the fit line given by (4) is in red.

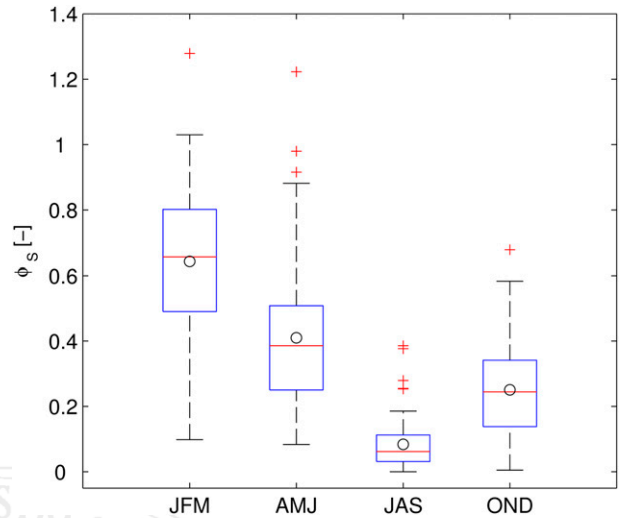


FIG. 6. Seasonal runoff coefficient $\phi_S$ historical statistics at the Flumendosa basin. Each box indicates the seasonal runoff coefficient statistics, the red solid line indicates the median, the black circle indicates the mean, the box and whiskers represent quartiles, and outliers are depicted individually. The seasons are January–March (JFM), April–June (AMJ), July–September (JAS), and October–December (OND).

$$\hat{\phi}_{Y_2} = a_2\,\mathrm{Std}(P_M)^{-1} + b_2, \tag{7}$$

where $\hat{\phi}_{Y_2}$ is the value of $\phi_Y$ estimated using $\mathrm{Std}(P_M)$ and (7), and $a_2$ and $b_2$ are the regression coefficients ($a_2 = -14.81$ mm and $b_2 = 0.67$). The value of $R^2$ is 0.52 while the RMSE value is 0.09. In years with high runoff coefficients, the monthly rain distribution tends to be less uniform and more concentrated in a small subset of months (i.e., high time variability, Fig. 7). Hence, the precipitation seasonality may be an important term impacting the runoff coefficient dynamics.

### b. *Precipitation seasonality impact on runoff generation*

The standard deviation of monthly precipitation is not enough for representing the precipitation seasonality because it does not distinguish between different types of seasonality, such as one concentrated during a several-month-long single rainy season versus alternating wet and dry months. It does not allow us to identify the period of the year with the highest precipitation; it just allows us to depict the rain uniformity during the year. The seasonality index of Markham (1970) is more useful for evaluating the precipitation seasonality, because it indicates both the degree of seasonal concentration and the period of the year with high rain. Therefore, SI seems attractive for evaluating the relationship between the precipitation seasonality and the runoff coefficient. We detect an interesting relationship (Fig. 8) between SI and the residuals of the runoff coefficient $[\delta\phi_{Y_1} = \phi_Y - \hat{\phi}_{Y_1}(P_Y)]$ that are the difference between the observed values of $\phi_Y$ and the polynomial fit line $\hat{\phi}_{Y_1}(P_Y)$ provided by (6) (Fig. 5) based on annual precipitation. This residual relationship ($R^2 = 0.31$ and RMSE $= 0.07$) is described as

$$\delta\hat{\phi}_Y = a_3\,\mathrm{SI}^{b_3} + c_3, \tag{8}$$

with the $a_3$, $b_3$, and $c_3$ coefficients equal to 0.45, 0.5, and $-0.27$, respectively. Note that SI is strongly related to the rainfall seasonality, such as can be evinced, for instance, by its relationship with the day of the year when the 70% of the total yearly rain is reached $P_{70}$, reaching a high correlation coefficient of $-0.76$ (scatterplot is inset in Fig. 8), much higher than the correlation coefficient ($= -0.55$) between $\mathrm{Std}(P_M)$ and $P_{70}$. The use of SI allows us to well depict yearly runoff changes. Indeed, when we use (8) for accounting for precipitation seasonality effects, yearly runoff can be well predicted. We compare $Q_Y$ estimates from $P_Y$ observations using 1) the nonlinear relationship between $\phi_Y$ and $P_Y$, that is $Q_{Y_1} = \hat{\phi}_{Y_1}P_Y$, with $\hat{\phi}_{Y_1}(P_Y)$, provided by (6), and 2) adding the SI effect on the runoff coefficient, estimated by (8), that is $Q_{Y_2} = \hat{\phi}_{Y_1}P_Y + \delta\hat{\phi}_Y(\mathrm{SI})P_Y$. We compare the $Q_{Y_1}$ and $Q_{Y_2}$ estimates with the yearly runoff observations: when the runoff model includes the simple proposed SI correction ($Q_{Y_2}$ model) the runoff estimates improved [the RMSE decreases from 70.5 to 59.1 mm, and the Nash and Sutcliffe (1970) model efficiency increases from 0.81 to 0.87]. Hence, with this analysis we notice that



Fig(s). 6,5 live 4/C

JOBNAME: JHM 00#00 2018 PAGE: 8 SESS: 8 OUTPUT: Mon Feb 19 16:26:24 2018 Total No. of Pages: 14
/ams/jhm/0/jhmD170078



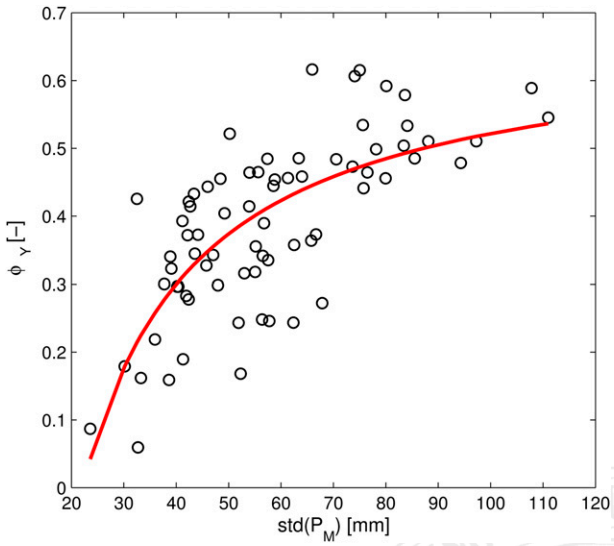


FIG. 7. The annual runoff coefficient $\phi_Y$ plotted relationship with the standard deviation of the monthly rainfall of each year [Std($P_M$)]. The fitted line given by (5) is in red.

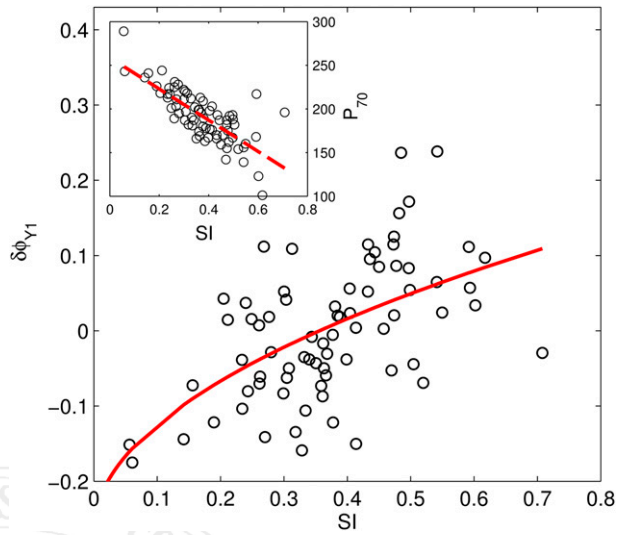


FIG. 8. The relationship between residuals from the annual runoff coefficient $\delta\phi_{Y1}$ and SI. The linear regression line ($\delta\hat{\phi}_Y = 0.45\text{SI}^{0.5} - 0.27$, $R^2 = 0.31$) is also reported in red. The inset shows the relationship between $P_{70}$ and SI (the linear regression line is in red with equation $P_{70} = -179\text{SI} + 258.8$, $R^2 = 0.56$).

changes in seasonality have a strong impact on yearly runoff. In the following we will investigate the persistence and trends of the seasonality changes.

### c. Seasonal hydrological trends

Because of the high impact of the rainfall seasonality on the surface runoff, we investigate potential trends in the seasonality of precipitation. The preferential decrease of precipitation in the wet months of the Flumendosa basin is shown in Fig. 9. We compared the precipitation regimes from before and after 1975, which is the starting year of the long drought in the Flumendosa basin.

The decrease of the precipitation is relevant from October to March, while almost no effects were detected during spring and summer months (Fig. 9). The reduction of the winter and autumn monthly precipitation even more drastically affected the surface runoff (Fig. 9) because of the strong precipitation elasticity of streamflow in this typical Mediterranean basin.

Winter precipitation strongly decreased (Table 1) with $\tau$ of $-0.21$ ($p = 0.007$) and a trend line slope (estimated using the TSA method) of $-0.48$ mm yr$^{-1}$. In the other seasons the decrease of precipitation is lower, even increasing slightly in spring and summer. Because of the impact of winter precipitation on runoff, the winter runoff also strongly decreased ($\tau = -0.23$, $p = 0.0045$, and a slope of $-0.48$ mm yr$^{-1}$, Table 1) but also the autumn and summer runoff trends decreased significantly ($\tau = -0.2$ and $-0.22$, and trend slopes of $-0.26$ and $-0.02$, respectively), so that the runoff trend is negative for all the seasons.

Yearly runoff is decreasing at a faster rate than the yearly precipitation decrease (normalized slope of the runoff trend $\beta_{Q_Y}/\overline{Q}_Y$ is $-8.7‰$ while that of the precipitation trend $\beta_{P_Y}/\overline{P}_Y$ is $-2.2‰$; Table 1). This is largely due to the high precipitation elasticity to streamflow. Also, we note that $Q_Y$ is produced mainly in winter (51%, Table 1) and autumn (26%, Table 1), during which the precipitation elasticity to streamflow is greater than 1, and $\beta_Q/\overline{Q}$ is greater (in a negative sense) than $\beta_P/\overline{P}$ (in winter almost double and in autumn more than double; Table 1). There is a notable weakening of the seasonal structure in precipitation here, which is marked by a reduction of precipitation in the seasons with a high runoff coefficient (autumn and winter) and a modest increase in precipitation during the dry seasons with a low runoff coefficient. The net effect is a magnification of the impacts on annual runoff.

The mean air temperature in the last three decades rose 0.05°C decade$^{-1}$ from June to September, while the changes are negligible during winter and spring.

### d. Large-scale pressure impact on the hydrological trends

Because the winter precipitation is the key season for runoff in the Flumendosa basin and a strong decrease trend is observed in the last decades, we look for the causes of the decrease. In this way, we can identify likely physical controls that explain the winter precipitation decline, with the goal that future drops of runoff become potentially predictable. As a starting point (Hurrell and

JOBNAME: JHM 00#00 2018 PAGE: 9 SESS: 8 OUTPUT: Mon Feb 19 16:26:24 2018 Total No. of Pages: 14
/ams/jhm/0/jhmD170078



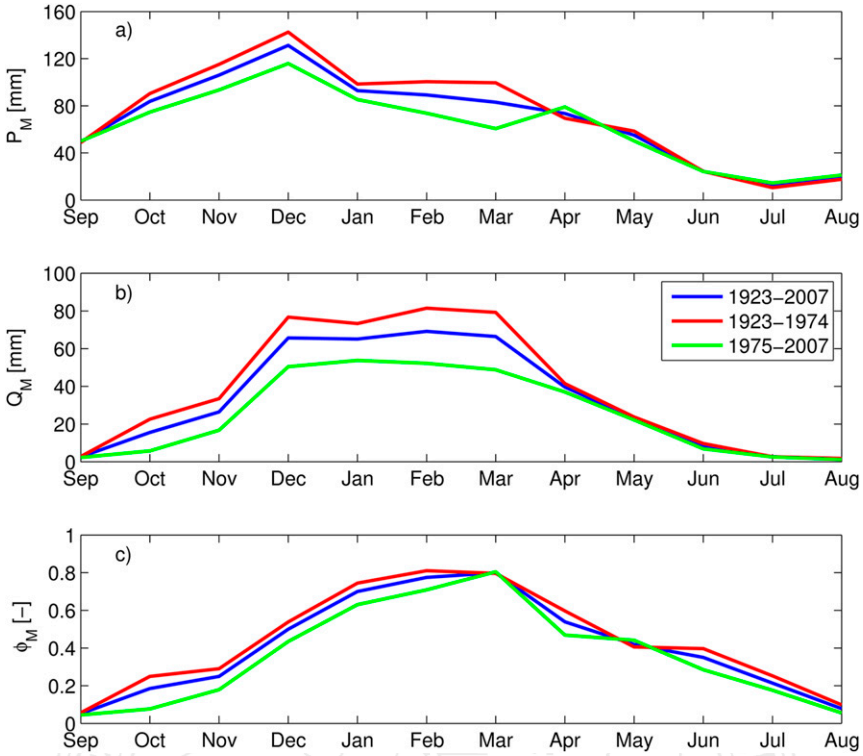


FIG. 9. Seasonal regimes of (a) monthly rainfall $P_M$, (b) runoff $Q_M$, and (c) runoff coefficient $\phi_M$ for the three periods (1923–74, 1975–2007, and 1923–2007).

Van Loon 1997; Trigo et al. 2000), we investigate the correlation of the extended winter (from December to March) NAO ($NAO_W$) with the extended winter precipitation $P_W$. The $NAO_W$ and $P_W$ are significantly negative correlated ($\rho = -0.5$, $R^2 = 0.2$, $p < 0.01$; F10 T2 Fig. 10a, Table 2), confirming that the recent positive phase of NAO during winter (Hurrell 1995) produced drier climate conditions in the Mediterranean basin, and, hence, the rainfall decrease. The correlation coefficient between $NAO_W$ and the extended winter runoff $Q_W$ is also high ($= -0.45$ with $R^2 = 0.2$; Table 2, Fig. 10b). The connection of $P_W$ and $Q_W$ with large-scale pressure indices increases when the correlations with MOI_1 and MOI_2 are investigated due to the natural stronger connections of precipitation and runoff dynamics with local pressure oscillations (Table 2).

### *e. Implications for hydrological planning and design*

The significant decreasing trends of rain and runoff may impact the hydrological design criteria for water resources planning. In this sense we investigate the impact of this historical climate change on the DSI for drought design and water resources planning (~~Yievchev~~, 1967; Dracup et al. 1980; Clausen and Pearson 1995).

We can anticipate an increase of drought intensity and frequency. Droughts are produced by extended periods, from seasons to years, of a deficiency in precipitation (Mishra and Singh 2010; Wanders and Wada 2015). A frequency analysis of the DSI is provided using the Gumbel distribution (Zelenhasić and Salvai 1987) distinguishing the whole study period and the two subperiods (1924–74 and 1975–2007), and for the return periods of 50, 100, 200, 300, and 500 years (Fig. 11; F11 statistics of the Kolmogorov–Smirnov and chi-squared tests for normality applied to the DSI time series are in Table 3). DSI drastically increases (≈65%) for all the T3 return periods in the last three decades (Fig. 11). Hence, based on the historical runoff data, droughts in the Flumendosa basin are increasing in severity, and this climate change effect must be significantly considered for water resources planning.

## 4. Conclusions

Through a detailed analysis of the hydrological processes in the Flumendosa basin, we explored the climate tendencies over this area, which could be considered the most important in Sardinia from the water resources management view point. Interestingly, the historical yearly runoff decrease has been more pronounced than the yearly precipitation decrease, highlighting a high elasticity of streamflow of 2.18. Indeed, from 1975 a

JOBNAME: JHM 00#00 2018 PAGE: 10 SESS: 8 OUTPUT: Mon Feb 19 16:26:25 2018 Total No. of Pages: 14
/ams/jhm/0/jhmD170078



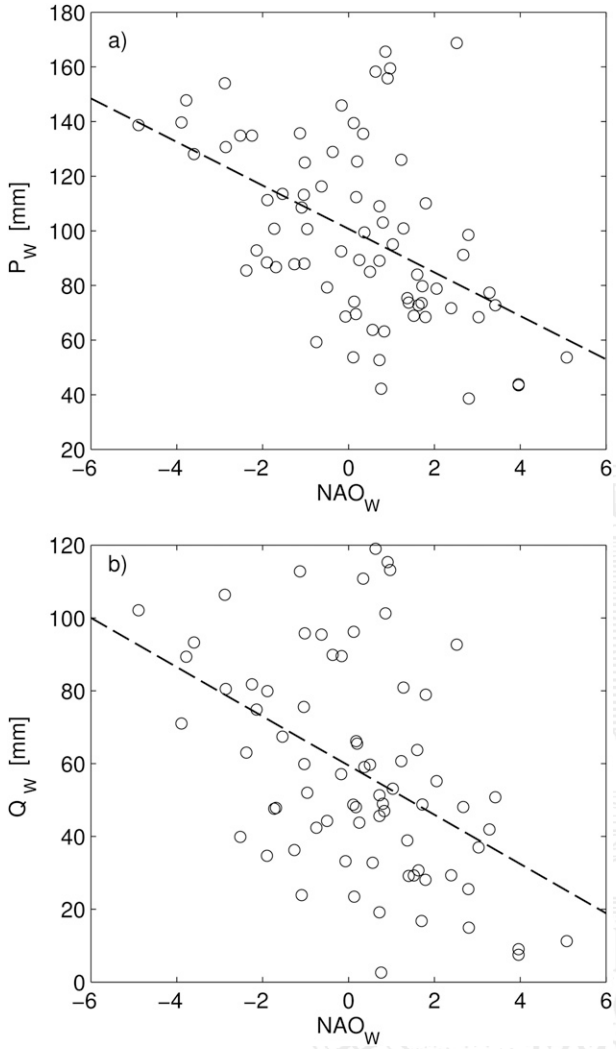


FIG. 10. Relationships between $NAO_W$ and (a) the extended winter precipitation $P_W$ and (b) the extended winter runoff $Q_W$. The regression lines ($P_W = -7.96NAO_W + 100.69$ with $R^2 = 0.25$, and $Q_W = -6.76NAO_W + 59.47$ with $R^2 = 0.2$) are the black dotted lines.

sequence of dry periods has affected the Flumendosa basin with dramatic impact on agricultural water use and even domestic water use of the island's largest city, Cagliari. Unlike some other efforts (Roderick and Farquhar 2011; Zhou et al. 2016), the changes of yearly runoff in the Flumendosa basin cannot be explained because of changes in climate through a first-order Taylor approximation alone, because of the importance of interannual variability in rainfall seasonality.

The precipitation mainly decreased during the winter months when the wet soil humidity conditions and the atmospheric conditions (lower evaporative demand) generally produce high surface runoff. The role of seasonal precipitation on Flumendosa hydrology was revealed in this study through the analyses of the seasonality index of Markham (1970) and its relationship with the surface runoff. The seasonality is a key term for the surface runoff process, and the estimate of annual runoff amounts through a simple model improves when the precipitation seasonality effect is involved.

TABLE 2. Correlation coefficients for the winter extend period (from December to March) between climate indices (NAO, MOI_1, and MOI_2) and precipitation and runoff.

| | $NAO_W$ | MOI_1 | MOI_2 |
|---|---|---|---|
| $P_W$ | −0.50 | −0.56 | −0.55 |
| $Q_W$ | −0.45 | −0.47 | −0.46 |

A significant negative correlation was found between winter precipitation and the NAO, when the NAO has a strong impact on Mediterranean climate. The high correlation value (= −0.5) is consistent with the Hurrell (1995) estimate (= −0.48) at Ajaccio in Corsica (northern Sardinia) and the Delitala et al. (2000) estimate (= −0.50 between the NAO and a Sardinian mean standardized anomaly precipitation index), while it slightly differs from the Brunetti et al. (2000) estimate AU6 of −0.37, but this was an average of stations on the two main Italian islands and considered only three Sardinian stations on the south and north Sardinian coast. However, the results confirm the sensitivity of this Mediterranean local area to global climate changes and that the Mediterranean climate is one of the ''hot spots'' of future climate change (Giorgi 2006; Diffenbaugh and Giorgi 2012).

Considering the increase of the predictability of the winter NAO (Scaife et al. 2014; Smith et al. 2016), there is the opportunity to predict future winter precipitation and runoff tendencies. The link between circulation patterns and precipitation during the winter period in the Mediterranean area has been predicted for the future by Beranová and Kyselý (2016). The persistence of a positive NAO over the Mediterranean area is predicted for the future (Ulbrich and Christoph 1999; Pinto et al. 2007), which will potentially have a consequent decrease in winter precipitation and an increase of dryness in the Flumendosa basin, with dramatic effects on agriculture and water resources for the whole of southern Sardinia, such as shown in a smaller Sardinia basin by Piras et al. (2014).

These results are currently affecting and will continue to affect the future hydrologic design from the water resources planning perspective. Using the DSI, we identified and characterized the hydrological droughts, estimating an increase of drought severity of about 65% over the last 30 years for the return periods of 50, 100, 200, 300, and 500 years, which may be further amplified

JOBNAME: JHM 00#00 2018 PAGE: 11 SESS: 8 OUTPUT: Mon Feb 19 16:26:25 2018 Total No. of Pages: 14
/ams/jhm/0/jhmD170078



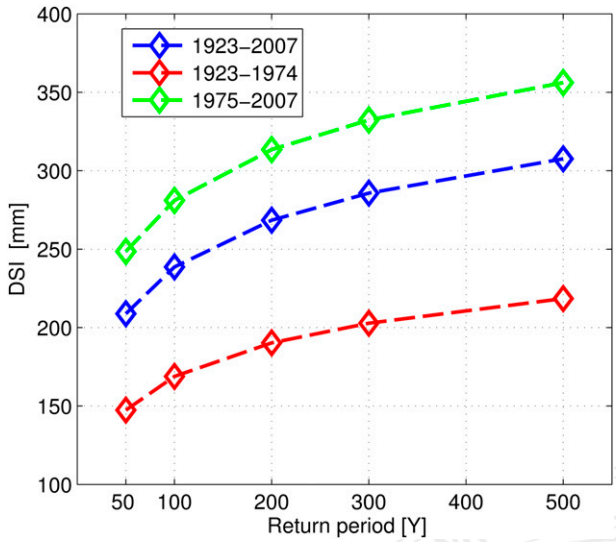


FIG. 11. Climate change implications for hydrologic design. DSI for the three periods (1923–74, 1975–2007, and 1923–2007) and for the return periods of 50, 100, 200, 300, and 500 years.

according to NAO future scenarios. Although the results are for a specific Mediterranean area, the results can be considered representative for all the Mediterranean regions.

The importance of the results and the need to understand climate change effects on local hydrology is confirmed by the European Union Commission that called member states to develop drought risk management plans (European Commission 2007). Water scarcity and droughts have emerged as a major challenge, and climate change is expected to make matters worse all over the world. In this sense the European Commission specifies that, in a context where climate changes contribute to an increase in the likelihood and the adverse impacts of dry periods, high-quality knowledge and information on the extent of the challenge and projected trends need to be considered for water resources and planning activities and the development of drought risk management strategies. In this context, research, such as we have proposed, has a significant role in providing knowledge and support to policy making.

TABLE 3. Results of the statistics tests (chi-squared and Kolmogorov–Smirnov tests) of the Gumbel distribution fitting to the DSI time series of the Flumendosa basin for the three considered periods (1923–2007, 1923–74, and 1975–2007). Statistics of the chi-squared and Kolmogorov–Smirnov tests for normality applied to the series have 5% significance level.

| Period | Kolmogorov–Smirnov | Chi-squared |
|---|---|---|
| 1923–2007 | 0.0874 | 6.01[a] |
| 1923–74 | 0.013 05 | 0.38[b] |
| 1975–2007 | 0.0883 | 2.58[c] |

[a] For $a = 0.05$, degrees of freedom = 4, the critical region is Xcr > 9.4877. For $a = 0.01$, degrees of freedom = 4, the critical region is Xcr > 13.2767.

[b] For $a = 0.05$, degrees of freedom = 1, the critical region is Xcr > 3.8415. For $a = 0.01$, degrees of freedom = 1, the critical region is Xcr > 6.6349.

[c] For $a = 0.05$, degrees of freedom = 1, the critical region is Xcr > 3.8415. For $a = 0.01$, degrees of freedom = 1, the critical region is Xcr > 6.6349.

*Acknowledgments.* This work was supported by the Regione Sardegna LR 7/2007 through Grant CRP-79793 for the "IDROSAR" research project and by the Ente Acque della Sardegna (Cagliari, Italy) and Regione Sardegna through the LR 19/2006. We thank the Sardinian Regional Hydrographic Service for providing some of the hydrologic data. Albertson was supported by the National Science Foundation through grants EAR-08-38301 and ECCS-1556900. Finally, we thank two anonymous reviewers for their useful comments and suggestions.

## APPENDIX A

### Mann–Kendall Test

Trend analysis is largely employed to understand the behavior of hydrological time series like rainfall and runoff. The nonparametric MK test is less sensitive to extremes than parametric trend detection tests and for this reason has been applied widely in hydrological studies (Helsel and Hirsch 2002).

The value of $\tau$ (Kendall 1938, 1975), resulting from the application of the MK test, measures the relationship between two $x$ and $y$ series. The MK test is based on the statistic $S$, obtained by subtracting the number of discordant pairs $M$, from the number of $(x,y)$ $P$ pairs where $y$ increases with increasing $x$:

$$S = P - M. \tag{A1}$$

The value of $\tau$ is defined as

$$\tau = \frac{S}{m(m-1)/2}, \tag{A2}$$

where $m$ represents the number of data pairs, and $\tau$ is a number falling between $-1$ and $+1$.

The significance of $\tau$ is tested by comparing $S$ to what would be expected when the null hypothesis is true: if it is further from 0 than expected, the null hypothesis is rejected.

When $n > 10$, the test statistic $S$ is modified to follow a standard normal distribution. Parameter $Z_s$ is defined as

$$Z_S = \begin{cases} \dfrac{S-1}{\sigma_S} & \text{if} \quad S \geq 0 \\ 0 & \text{if} \quad S = 0\,, \\ \dfrac{S+1}{\sigma_S} & \text{if} \quad S < 0 \end{cases} \tag{A3}$$

where

$$\sigma_S = \sqrt{\frac{m(m-1)(2m+5)}{18}}. \tag{A4}$$

The null hypothesis is rejected at significance level $\alpha$ if $|Z_s| > Z_{\text{crit}}$, where $Z_{\text{crit}}$ is the value of the standard normal distribution with a probability of exceedance of $\alpha/2$: the values of $x$ and/or $y$ are tied and a correction on the $\sigma_s$ must be applied. In the case where some values of $x$ and/or $y$ are tied, the formula for $\sigma_s$ is corrected as follows (Helsel and Hirsch 2002):

$$\sigma_s = \sqrt{\frac{m(m-1)(2m+5) - \sum_{i=1}^{m} t_i(i)(i-1)(2i+5)}{18}}, \tag{A5}$$

where $t_i$ is the number of ties of extent $i$.

## APPENDIX B

### Theil–Sen Approach

The Theil–Sen method uses a linear model to estimate the slope of the trend (Theil 1950; Sen 1968, and the variance of the residuals should be constant in time calculated as

$$Q_i = \frac{X_j - X_k}{j-k} \quad \text{for} \quad i = 1, \ldots, l, \tag{B1}$$

where $X_j$ and $X_k$ are the data values at times $j$ and $k$ ($j > k$), respectively. If there is only one datum in each time period, then $L = l(l-1)/2$, where $l$ is the number of time periods. If there are multiple observations in one or more time periods, then $L < l(l-1)/2$. The $l$ values of $Q_i$ are ranked from smallest to largest, and the median of the slope or Sen's slope estimator is computed as

$$\beta = \begin{cases} Q_{[(l+1)/2]}, & \text{if} \quad l \text{ is odd} \\ \dfrac{Q_{(l/2)} + Q_{[(n+2)/2]}}{2}, & \text{if} \quad l \text{ is even} \end{cases}. \tag{B2}$$

The $\beta$ sign reflects the data trend, while its value indicates the steepness of the trend.

The Theil–Sen method and the Mann–Kendall test are strongly connected; the $\beta$ slope estimator is related to the Mann–Kendall $\tau$ test statistic, such that if $\tau < 0$ then $\beta \leq 0$, and if $\tau > 0$, then $\beta \geq 0$ because $\tau$ is equivalent to the number of positive $S$ [(A1)] minus the number of negative $S$, and $\beta$ is the median of these $S$.

## REFERENCES

Altın, T. B., and B. Barak, 2014: Changes and trends in total yearly precipitation of the Antalya District, Turkey. *Procedia Soc. Behav. Sci.*, **120**, 586–599, https://doi.org/10.1016/j.sbspro.2014.02.139.

Barry, R. G., and R. J. Chorley, 1992: Atmosphere, Weather and Climate. 6th ed. Routledge, 392 pp.

Beniston, M., and Coauthors, 2007: Future extreme events in European climate: An exploration of regional climate model projections. *Climatic Change*, **81**, 71–95, https://doi.org/10.1007/s10584-006-9226-z.

Beranová, R., and J. Kyselý, 2016: Links between circulation indices and precipitation in the Mediterranean in an ensemble of regional climate models. *Theor. Appl. Climatol.*, **123**, 693–701, https://doi.org/10.1007/s00704-015-1381-6.

Brandimarte, L., G. G. Baldassarre, G. Bruni, P. D'Odorico, and A. Montanari, 2011: Relation between the North-Atlantic Oscillation and hydroclimatic conditions in Mediterranean areas. *Water Resour. Manage.*, **25**, 1269–1279, https://doi.org/10.1007/s11269-010-9742-5.

Brunetti, M., M. Colacino, M. Maugeri, and T. Nanni, 2001: Trends in the daily intensity of precipitation in Italy from 1951 to 1996. *Int. J. Climatol.*, **21**, 299–316, https://doi.org/10.1002/joc.613.

——, M. Maugeri, and T. Nanni, 2002: Atmospheric circulation and precipitation in Italy for the last 50 years. *Int. J. Climatol.*, **22**, 1455–1471, https://doi.org/10.1002/joc.805.

Cao, C., R. Silvano, and A. Fadda, 1998: Nuovo Studio dell'idrologia superficiale della Sardegna. Ente Autonomo del Flumendosa, XX pp. AU7

Chang, T. J., and J. R. Stenson, 1990: Is it realistic to define a 100-year drought for water management. *Water Resour. Bull.*, **26**, 823–829, https://doi.org/10.1111/j.1752-1688.1990.tb01416.x.

Chiew, F. H. S., W. J. Young, and W. Cai, 2011: Current drought and future hydro-climate projection in Southeast Australia and implication for water management. *Stochastic Environ. Res. Risk Assess.*, **25**, 601–612, https://doi.org/10.1007/s00477-010-0424-x.

Choudhury, B. J., 1999: Evaluation of an empirical equation for annual evaporation using field observations and results from a biophysical model. *J. Hydrol.*, **216**, 99–110, https://doi.org/10.1016/S0022-1694(98)00293-5.

Clausen, B., and C. P. Pearson, 1995: Regional frequency analysis of annual maximum streamflow drought. *J. Hydrol.*, **173**, 111–130, https://doi.org/10.1016/0022-1694(95)02713-Y.

Conte, M., S. Giuffrida, and S. Tedesco, 1989: The Mediterranean oscillation: Impact on precipitation and hydrology in Italy. *Proceedings of the Conference on Climate and Water*, Publications of the Academy of Finland, 121–137.

Dai, A., K. E. Trenberth, and T. Qian, 2004: A global dataset of Palmer drought severity index for 1870–2004: Relationship with soil moisture and effects of surface warming. *J. Hydrometeor.*, **5**, 1117–1130, https://doi.org/10.1175/JHM-386.1.

Delitala, A. M. S., D. Cesari, P. A. Chessa, and M. N. Ward, 2000: Precipitation over Sardinia (Italy) during the 1946–1993 rainy seasons and associated large-scale climate variations. *Int. J. Climatol.*, **20**, 519–541, https://doi.org/10.1002/(SICI)1097-0088(200004)20:5<519::AID-JOC486>3.0.CO;2-4.

Detto, M., N. Montaldo, J. D. Albertson, M. Mancini, and G. Katul, 2006: Soil moisture and vegetation controls on evapotranspiration in an heterogeneous Mediterranean ecosystem on Sardinia, Italy. *Water Resour. Res.*, **42**, W08419, https://doi.org/10.1029/2005WR004693.

Diffenbaugh, N. S., and F. Giorgi, 2012: Climate change hotspots in the CMIP5 global climate model ensemble. *Climatic Change*, **114**, 813–822, https://doi.org/10.1007/s10584-012-0570-x.

Dingman, S. L., 2015: *Physical Hydrology*. 3rd ed. Waveland Press, 643 pp.

Doblas-Miranda, E., and Coauthors, 2015: Reassessing global change research priorities in mediterranean terrestrial ecosystems: How far have we come and where do we go from here? *Global Ecol. Biogeogr.*, **24**, 25–43, https://doi.org/10.1111/geb.12224.

Dracup, J. A., K. S. Lee, E. G. Paulson jr., 1980: On the definition of droughts. *Water Resour. Res.*, **16**, 297–302, https://doi.org/10.1029/WR016i002p00297.

Dunkeloh, A., and J. Jacobeit, 2003: Circulation dynamics of Mediterranean precipitation variability 1948–98. *Int. J. Climatol.*, **23**, 1843–1866, https://doi.org/10.1002/joc.973.

European Commission, 2007: Addressing the challenge of water scarcity and droughts. COM(2007)414, 14 pp., http://eur-lex.europa.eu/LexUriServ/LexUriServ.do?uri=COM:2007:0414:FIN:EN:PDF.

Gao, P., X. M. Mu, F. Wang, and R. Li, 2011: Changes in streamflow and sediment discharge and the response to human activities in the middle reaches of the Yellow River. *Hydrol. Earth Syst. Sci.*, **15**, 1–10, https://doi.org/10.5194/hess-15-1-2011.

García-Ruiz, J. M., J. I. López-Moreno, S. M. Serrano-Vicente, S. Beguería, and T. Lasanta, 2011: Mediterranean water resources in a global change scenario. *Earth Sci. Rev.*, **105**, 121–139, https://doi.org/10.1016/j.earscirev.2011.01.006.

Giorgi, F., 2006: Climate change hot-spots. *Geophys. Res. Lett.*, **33**, L08707, https://doi.org/10.1029/2006GL025734.

Helsel, D. R., and R. M. Hirsch, 2002: Statistical methods in water resources. Hydrologic Analysis and Interpretation, Book 4, Techniques of Water-Resources Investigations of the United States Geological Survey, 522 pp., https://pubs.usgs.gov/twri/twri4a3/.

Hurrell, J. W., 1995: Decadal trends in the North Atlantic Oscillation: Regional temperatures and precipitation. *Science*, **269**, 676–679, https://doi.org/10.1126/science.269.5224.676.

——, 1996: Influence of variations in extratropical wintertime teleconnections on northern hemisphere temperature. *Geophys. Res. Lett.*, **23**, 665–668, https://doi.org/10.1029/96GL00459.

——, and H. Van Loon, 1997: Decadal variations associated with the North Atlantic Oscillation. *Climatic Change*, **36**, 301–326, https://doi.org/10.1023/A:1005314315270.

Jaiswal, R. K., K. Lohani, and H. L. Tiwari, 2015: Statistical analysis for change detection and trend assessment in climatological parameters. *Environ. Processes*, **2**, 729–749, https://doi.org/10.1007/s40710-015-0105-3.

Kendall, M. G., 1938: A new measure of rank correlation. *Biometrika*, **30**, 81–93, https://doi.org/10.1093/biomet/30.1-2.81.

——, 1975: *Rank Correlation Methods*. 4th ed. Charles Griffin, 202 pp.

Lespinas, F., W. Ludwig, and S. Heussner, 2010: Impact of recent climate change on the hydrology of coastal Mediterranean rivers in southern France. *Climatic Change*, **99**, 425–456, https://doi.org/10.1007/s10584-009-9668-1.

Lionello, P., and Coauthors, 2006: Cyclones in the Mediterranean region: Climatology and effects on the environment. *Dev. Earth Environ. Sci.*, **4**, 325–372, https://doi.org/10.1016/S1571-9197(06)80009-1.

López-Moreno, J. I., M. Beniston, and J. M. García-Ruiz, 2008: Environmental change and water management in the Pyrenees: Facts and future perspectives for Mediterranean mountains. *Global Planet. Change*, **61**, 300–312, https://doi.org/10.1016/j.gloplacha.2007.10.004.

——, S. M. Vicente-Serrano, E. Morán-Tejeda, J. Lorenzo-Lacruz, A. Kenawy, and M. Beniston, 2011: Effects of the North Atlantic Oscillation (NAO) on combined temperature and precipitation winter modes in the Mediterranean mountains: Observed relationships and projections for the 21st century. *Global Planet. Change*, **77**, 62–76, https://doi.org/10.1016/j.gloplacha.2011.03.003.

Lorenzo-Lacruz, J., S. M. Vicente-Serrano, J. I. López-Moreno, E. Morán-Tejeda, and J. Zabalza, 2012: Recent trends in Iberian streamflows (1945–2005). *J. Hydrol.*, **414–415**, 463–475, https://doi.org/10.1016/j.jhydrol.2011.11.023.

Maidment, D. R., 1993: *Handbook of Hydrology*. McGraw-Hill, 1424 pp.

Manara, V., M. Brunetti, A. Celozzi, M. Maugeri, A. Sanchez-Lorenzo, and M. Wild, 2016: Detection of dimming/brightening in Italy from homogenized all-sky and clear-sky surface solar radiation records and underlying causes (1959–2013). *Atmos. Chem. Phys.*, **16**, 11145–11161, https://doi.org/10.5194/acp-16-11145-2016.

Mariotti, A., N. Zeng, J.-H. Yoon, V. Artale, A. Navarra, P. Alpert, and L. Z. X. Li, 2008: Mediterranean water cycle changes: Transition to drier 21st century conditions in observations and CMIP3 simulations. *Environ. Res. Lett.*, **3**, 044001, https://doi.org/10.1088/1748-9326/3/4/044001.

Markham, C. G., 1970: Seasonality of precipitation in the United States. *Ann. Assoc. Amer. Geogr.*, **60**, 593–597, https://doi.org/10.1111/j.1467-8306.1970.tb00743.x.

Martínez-Fernández, J., N. Sánchez, and C. M. Herrero-Jiménez, 2013: Recent trends in rivers with near-natural flow regime: The case of the river headwaters in Spain. *Prog. Phys. Geogr.*, **37**, 685–700, https://doi.org/10.1177/0309133313496834.

May, W., 2008: Potential future changes in the characteristics of daily precipitation in Europe simulated by the HIRHAM regional climate model. *Climate Dyn.*, **30**, 581–603, https://doi.org/10.1007/s00382-007-0309-y.

Mishra, A. K., and V. P. Singh, 2010: A review of drought concepts. *J. Hydrol.*, **391**, 202–216, https://doi.org/10.1016/j.jhydrol.2010.07.012.

AU8 Montaldo, N.J. D. AlbertsonM. Mancini, 2010: Vegetation dynamics and soil water balance in a water-limited Mediterranean ecosystem on Sardinia, . *Italy. Hydrol. Earth Syst. Sci.*, **12**, 1257–1271, https://doi.org/10.5194/hess-12-1257-2008.

——R. CoronaJ. D. Albertson, 2013: On the separate effects of soil and land cover on Mediterranean ecohydrology: Two contrasting case studies in Sardinia, . *Italy. Water Resour. Res.*, **49**, 1123–1136, https://doi.org/10.1029/2012WR012171.

Nash, J. E., and J. V. Sutcliffe, 1970: River flow forecasting through conceptual models. Part I—A discussion of principles. *J. Hydrol.*, **10**, 282–290, https://doi.org/10.1016/0022-1694(70)90255-6.

Osborn, T. J., K. R. Briffa, S. F. B. Tett, P. D. Jones, and R. M. Trigo, 1999: Evaluation of the North Atlantic Oscillation as simulated by a coupled climate model. *Climate Dyn.*, **15**, 685–702, https://doi.org/10.1007/s003820050310.

Ozturk, T., Z. P. Ceber, M. Türkeş, and M. L. Kurnaz, 2015: Projections of climate change in the Mediterranean Basin by using downscaled global climate model outputs. *Int. J. Climatol.*, **35**, 4276–4292, https://doi.org/10.1002/joc.4285.

Pettitt, A. N., 1979: A non-parametric approach to the change point problem. *Appl. Stat.*, **28**, 126–135, https://doi.org/10.2307/2346729.

Piervitali, E., M. Conte, and M. Colacino, 1999: Rainfall over the central-western Mediterranean basin in the period 1951–1995. Part II: Precipitation scenarios. *Nuovo Cimento*, **22** (5), 649–661.

Pinto, J. G., U. Ulbrich, G. C. Leckebusch, T. Spangehl, M. Reyers, and S. Zacharias, 2007: Changes in storm track and cyclone activity in three SRES ensemble experiments with the ECHAM5/MPI-OM1 GCM. *Climate Dyn.*, **29**, 195–210, https://doi.org/10.1007/s00382-007-0230-4.

Piras, M., G. Mascaro, R. Deidda, and E.R. Vivoni, 2014: Quantification of hydrologic impacts of climate change in a Mediterranean basin in Sardinia, Italy, through high-resolution simulations. *Hydrol. Earth Syst. Sci.*, **18**, 5201–5217, https://doi.org/10.5194/hess-18-5201-2014.

Roderick, M. L., and G. D. Farquhar, 2011: A simple framework for relating variations in runoff to variations in climatic conditions and catchment properties. *Water Resour. Res.*, **47**, W00G07, https://doi.org/10.1029/2010WR009826.

Rojas, M., M. Rojas, L. Z. Li, M. Kanakidou, N. Hatzianastassiou, G. Seze, and H. Le Treut, 2013: Winter weather regimes over the Mediterranean region: Their role for the regional climate and projected changes in the twenty-first century. *Climate Dyn.*, **41**, 551–571, https://doi.org/10.1007/s00382-013-1823-8.

Romano, E., A. B. Petrangeli, and E. Preziosi, 2011: Spatial and time analysis of rainfall in the Tiber River basin (central Italy) in relation to discharge measurements (1920–2010). *Procedia Environ. Sci.*, **7**, 258–263, https://doi.org/10.1016/j.proenv.2011.07.045.

Sankarasubramanian, A., R. M. Vogel, and J. F. Limbrunner, 2001: Climate elasticity of streamflow in the United States. *Water Resour. Res.*, **37**, 1771–1781, https://doi.org/10.1029/2000WR900330.

Scaife, A. A., A. Arribas, E. Blockey, A. Brookshaw, R. T. Clark, and N. Dunstone, 2014: Skillful long-range prediction of European and North American winters. *Geophys. Res. Lett.*, **41**, 2514–2519, https://doi.org/10.1002/2014GL059637.

Schaake, J. C., and L. Chunzhen, 1989: Development and application of simple water balance models to understand the relationship between climate and water resources. *IAHS Publ.*, **181**, 343–352.

Sen, P. K., 1968: Estimates of the regression coefficient based on Kendall's tau. *J. Amer. Stat. Assoc.*, **63**, 1379–1389, https://doi.org/10.1080/01621459.1968.10480934.

Smith, D. M., A. A. Scaife, R. Eade, and J. R. Knight, 2016: Seasonal to decadal prediction of the winter North Atlantic Oscillation: Emerging capability and future prospects. *Quart. J. Roy. Meteor. Soc.*, **142**, 611–617, https://doi.org/10.1002/qj.2479.

Statzu, V. and E. Strazzera, 2009: Water demand for residential uses in a Mediterranean region: Econometric analysis and policy implications. University of Cagliari Working Paper, 31 pp., http://www.cide.info/conf/2009/iceee2009_submission_88.pdf.

Theil, H., 1950: A rank-invariant method for linear and polynomial regression analysis. *Proc. K. Ned. Akad. Wet., Ser. A*, **53**, 386–392, 512–525, 1397–1412.

Thiessen, A. H., 1911: Precipitation for large areas. *Mon. Wea. Rev.*, **39**, 1248–1254, https://doi.org/10.1175/1520-0493(1911)39<1248a:DNGB>2.0.CO;2.

Trigo, I. F., T. D. Davies, and G. R. Bigg, 2000: Decline in Mediterranean rainfall caused by weakening of Mediterranean cyclones. *Geophys. Res. Lett.*, **27**, 2913–2916, https://doi.org/10.1029/2000GL011526.

Trigo, R. M., and J. P. Palutikof, 2001: Precipitation scenarios over Iberia: A comparison between direct GCM output and different downscaling techniques. *J. Climate*, **14**, 4422–4446, https://doi.org/10.1175/1520-0442(2001)014<4422:PSOIAC>2.0.CO;2.

Ulbrich, U., and M. Christoph, 1999: A shift of the NAO and increasing storm track activity over Europe due to anthropogenic greenhouse gas forcing. *Climate Dyn.*, **15**, 551–559, https://doi.org/10.1007/s003820050299.

Vicente-Serrano, S. M., and Coauthors, 2011: The NAO impact on droughts in the Mediterranean region. *Hydrological, Socioeconomic and Ecological Impacts of the North Atlantic Oscillation in the Mediterranean Region*, S. M. Vicente-Serrano and R. Trigo, Eds., Advances in Global Change Research, Vol. 46, Springer, 23–40, https://doi.org/10.1007/978-94-007-1372-7_3.

Wanders, N., and Y. Wada, 2015: Human and climate impacts on the 21st century hydrological drought. *J. Hydrol.*, **526**, 208–220, https://doi.org/10.1016/j.jhydrol.2014.10.047.

Yang, H., J. Qi, X. Xu, D. Yang, and H. Lv, 2014:The regional variation in climate elasticity and climate contribution to runoff across China. *J. Hydrol.*, **517**, 607–616, https://doi.org/10.1016/j.jhydrol.2014.05.062.

Yevjevich, V., 1967: An objective approach to definition and investigation of continental hydrological droughts. Colorado State University Hydrology Papers 23, 19 pp., http://hdl.handle.net/10217/61303.

Zelenhasić, E., and A. Salvai, 1987: A method of streamflow analysis. *Water Resour. Res.*, **23**, 156–168, https://doi.org/10.1029/WR023i001p00156.

Zhang, S., and X. X. Lu, 2009: Hydrological responses to precipitation variation and diverse human activities in a mountainous tributary of the lower Xijiang, China. *Catena*, **77**, 130–142, https://doi.org/10.1016/j.catena.2008.09.001.

Zhou, S., B. Yu, L. Zhang, Y. Huang, M. Pan, and G. Wang, 2016: A new method to partition climate and catchment effect on the mean annual runoff based on the Budyko complementary relationship. *Water Resour. Res.*, **52**, 7163–7177, https://doi.org/10.1002/2016WR019046.